JOURNAL OF SYNCHROTRON RADIATION
ISSN 1600-5775

Received 2 March 2015
Accepted 14 June 2015

Edited by J. F. van der Veen

Keywords: polarimetry; monochromator; Compton scattering; X-ray diffraction; undulator high harmonics.

Influence of higher harmonics of the undulator in X-ray polarimetry and crystal monochromator design

Berit Marx-Glowna,[a]* Kai S. Schulze,[a,b] Ingo Uschmann,[a,b] Tino Kämpfer,[a,b] Günter Weber,[b,c] Christoph Hahn,[a,b] Hans-Christian Wille,[d] Kai Schlage,[d] Ralf Röhlsberger,[d] Eckhart Förster,[a,b] Thomas Stöhlker[b] and Gerhard G. Paulus[a,b]

[a]Institut für Optik und Quantenelektronik, Friedrich-Schiller-Universität Jena, Max-Wien-Platz 1, D-07743 Jena, Germany, [b]Helmholtz-Institut Jena, Fröbelstieg 3, D-07743 Jena, Germany, [c]GSI Helmholtzzentrum für Schwerionenforschung, Planckstrasse 1, D-64291 Darmstadt, Germany, and [d]Deutsches Elektronen-Synchrotron DESY, Notkestrasse 85, D-22607 Hamburg, Germany. *Correspondence e-mail: berit.marx@uni-jena.de

The spectrum of the undulator radiation of beamline P01 at Petra III has been measured after passing a multiple reflection channel-cut polarimeter. Odd and even harmonics up to the 15th order, as well as Compton peaks which were produced by the high harmonics in the spectrum, could been measured. These additional contributions can have a tremendous influence on the performance of the polarimeter and have to be taken into account for further polarimeter designs.

1. Introduction

Recent developments in X-ray polarimetry make it possible to achieve polarization purities up to 10^{-10} (Marx *et al.*, 2013), where the polarization purity δ_0 is defined as the ratio of the integrated transmission T_π of the π-component to the integrated transmission T_σ of the σ-component (Alp *et al.*, 2000): $\delta_0 = T_\pi/T_\sigma$. These high purities have been achieved by using multiple reflections inside channel-cut crystals with Bragg angles of exactly 45° and by an optimized channel-cut orientation procedure (Marx *et al.*, 2011).

X-ray polarimetry has seen increasing attention in recent years. The initial development of X-ray crystal polarimeters started in the 1970s when Hart and Rodriguez advanced the crystal polarimeter and examined the polarization effects of solids in the X-ray regime (Hart, 1978; Hart & Rodrigues, 1979). The recent revival of interest in X-ray polarimetry was triggered by the use of polarimetry in nuclear resonant scattering (Siddons *et al.*, 1995, 1999; Alp *et al.*, 2000; Röhlsberger *et al.*, 1997; Heeg *et al.*, 2013), and also by other interesting applications in fundamental physics, such as the detection of vacuum birefringence (Heinzl *et al.*, 2006). In light of these and other interesting applications, it is important to develop X-ray polarimetry further and identify the limiting factors. These are, in fact, very small. However, for the high resolution and sensitivity of precise polarimeters, they need to be taken into account. Equally important are the properties of the X-ray radiation on which we concentrate in this paper. The spectrum transmitted by the polarimeter is analyzed in order to determine the influence of the incoming undulator radiation on the polarimeter.

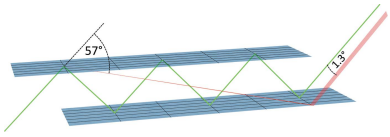

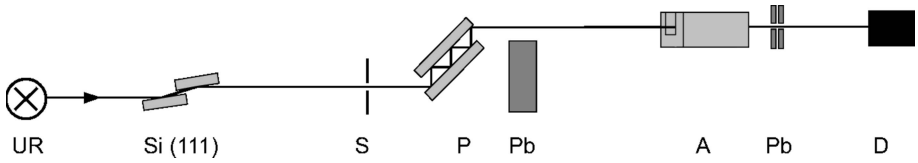

Figure 1
Experimental setup for the measurement of the polarimeter spectrum. UR: undulator radiation; Si (111): monochromator; S: slit; P: polarizer; Pb: lead shield; A: analyzer; D: detector.

2. Experiment

Measurement of the spectrum behind the polarimeter was performed at the high-resolution Dynamics Beamline P01 at Petra III in Hamburg. The experimental setup is shown in Fig. 1. The undulator U32 at P01 consists of two segments each 5 m long with 12.5 mm minimum gap. Using the third harmonic of the undulator, the photon energy was set to 12913.97 eV by an Si (111) double-crystal monochromator. The monochromator was not detuned to suppress the high harmonics. A channel-cut crystal with six symmetric Si (800) reflections was used to polarize the radiation. An equivalent channel-cut crystal was used as the analyzer and aligned 0.3° off the extinction position. The dimensions of the channel-cuts are 45 mm × 12 mm × 12 mm with a wall thickness of 3 mm. At the chosen photon energy, the Bragg angle for the Si (800) reflection lies at exactly 45°, which implies that the polarization component parallel to the diffraction plane of the crystal (π-component) is nearly fully suppressed. In order to shield the direct radiation from the monochromator and the transmitted part of the reflections of the polarizer, a lead brick was placed behind the polarizer crystal. Furthermore, two 0.5 mm-thick lead foils were attached to the analyzer to shield the direct radiation from the analyzer. The spectrum of the undulator radiation after passing the polarimeter was measured with a nitrogen-cooled lithium-drifted silicon (SiLi) photon spectrometer. The detector has an active diameter of 6 mm and is sensitive to a depth of 5.4 mm. The distance between analyzer and detector was about 40 cm. The spectrum shown in Fig. 2 was measured after an integration time of 1 h. During the measurement the synchrotron was working in the 240-bunch mode with a ring current of less than 100 mA.

3. Analysis of the spectrum

The spectrum (Fig. 2) shows sharp peaks at the 3rd, 9th, 12th and 15th harmonic of the undulator radiation. Random errors of the undulator and the emittance of the beam are known as a potential cause of on-axis even harmonics (Kincaid, 1985; Lai *et al.*, 1993). Multiphoton processes in the detector, on the other hand, can be excluded as a source of error, otherwise we would see peaks at the 6th and 8th harmonic as well. The intensity of the 12th harmonic is strong in comparison with the other even harmonics, because it can pass the monochromator. In addition, the spectrum displays Compton peaks for the 9th, 12th and 15th harmonics. The energy regions accessible for Compton scattered photons are indicated by the hatched grey areas. In Table 1, the Compton scattering angles for each energy are listed.

Concerning the question about the spatial origin of the peaks, we first note that the Compton peaks for all harmonics correspond to the same angular range. In addition, the peaks related to backscattering are stronger than those for forward scattering. Direct radiation from the undulator certainly cannot reach the detector because of the lead bricks. Therefore, one has to check whether these photons are scattered by Bragg reflections inside the channel-cut towards the detector. This was proven by simulations performed exemplarily for 33.7 keV and 37.5 keV as the number of strong reflections is lowest for the low-energy part of the spectrum. The orientation of the channel-cut crystals relative to the incident radiation was chosen in a way so that the angular distance to strong reflections is as large as possible (Marx *et al.*, 2013), as strong reflections can cause a decrease in intensity on the one hand and destroy the degree of linear polarization purity due to Umweg reflections on the other. For the chosen crystal azimuthal orientation of 14.7° relative to (010) and a direction of the incident wavevector of (0.71, 0.68, −0.18), the neighboring reflections are (224), (391), (71$\bar{1}$), (624), (11$\bar{5}$), (080) and (591). The simulations show that for this orientation of the crystals the Compton scattering can be excluded from taking place before the polarimeter and the scattering is not caused by the monochromator. There is no Bragg reflection in the polarizer crystal which hits the analyzer crystal at a distance of 1 m.

One remaining possible explanation is that the Compton scattering took place inside the channel-cut crystals and is diffracted towards the detector *via* Bragg reflections. If so, photons scattered in the channel-cut analyzer are much more

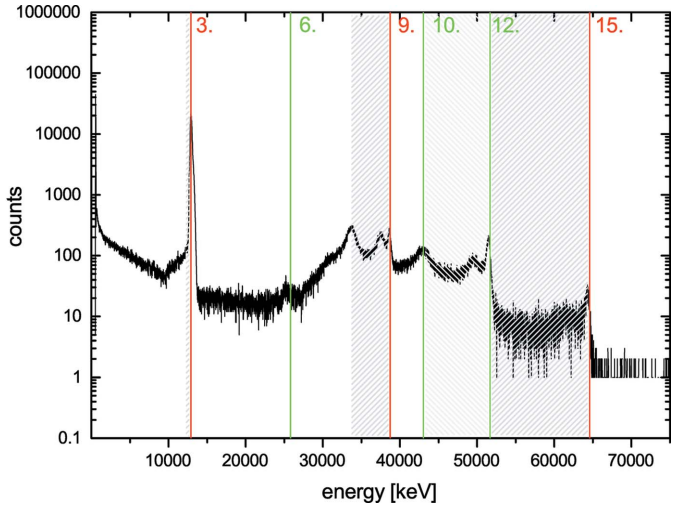

Figure 2
Measured polarimeter spectrum 0.3° off the extinction position. The red lines are the positions of the odd harmonics. The green lines describe the positions of the even harmonics. The hatched areas illustrate the regions where Compton scattering could take place.

Table 1
Measured photon energies and their related Compton scattering angles for the respective harmonics.

9th harmonic 38.74 keV		12th harmonic 51.66 keV		15th harmonic 64.57 keV	
33.7 keV	167°	43.0 keV	161°	51.6 keV	169°
37.5 keV	57°	49.5 keV	53°	61.4 keV	54°

likely to enter the detector because the solid angle of the detector is much larger for the analyzer. A simulation for all strong reflections shows that, out of a total of 13858 reflections, only the Si $(15, \bar{5}, \bar{1})$ reflection can hit the detector after Compton scattering at $\sim 57°$ of the incident radiation from the polarizer (see Fig. 3). For Compton scattering at $\sim 167°$, no Bragg reflection capable of reaching the detector was found. However, radiation transmitted by the polarizer and Compton scattered at the ceiling of the hutch is able to do so: the 1.4 m distance from the polarizer to the detector and the hutch height of 5.5 m result in a Compton scattering angle very close to 167°. These Compton scattered photons can easily be eliminated by a proper lead shielding in the future.

In total, more than half of all the photons detected (315 counts s^{-1}) can be found in the peak of the third harmonic (171 counts s^{-1}). This peak has a tail extending towards lower energies down to 9.5 keV which accounts for 6 counts s^{-1}. All higher harmonics contribute a total of 10 counts s^{-1}, all Compton peaks a total of 47 counts s^{-1}. The background has 87 counts s^{-1}. In addition, Compton scattering in the SiLi detector material has to be taken into account. In the following, we will see that the 47 counts s^{-1} of the Compton peaks can fairly easily be discriminated. Therefore, only Compton scattering of the harmonics in the SiLi detector was considered in a simulation. The result is 2.3 counts s^{-1} distributed in the background at energies lower than 20 keV.

4. Consequences on polarimetry

Now, the natural question is what effect these count rates will have on the achievable polarization purity. As mentioned at the beginning, the channel-cut crystals are optimized for a certain energy. The polarization purity at all other photon energies will decrease owing to a mismatch in Bragg angle or a rotation of the diffraction plane with respect to the main reflection. The best X-ray polarimeters can currently reach a polarization purity of $\delta_0 = 2.4 \times 10^{-10}$. Typical synchrotron sources provide 10^{10} to 10^{13} photons s^{-1}. For the present experiment, the number of photons available after the polarizer was 2×10^{10} photons s^{-1}, which was reduced to 8×10^{9} photons s^{-1} after the analyzer crystal in the passing direction (the polarizer crystal and the analyzer crystal are parallel to each other).

The considerable number of Compton scattered photons is independent of the Bragg angle of the analyzer. Therefore, these photons contribute to a constant background in rocking-curve measurements, which are always performed when

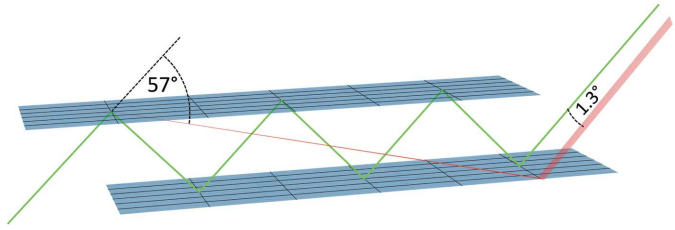

Figure 3
Drawing of the analyzer crystal. The incident radiation from the polarizer crystal (green line) from the left is Compton scattered at 57° (red line) and then Bragg reflected from Si $(15, \bar{5}, \bar{1})$ to the detector.

channel-cut polarimeters are used. For high purities, any background should be suppressed as much as possible in order to successfully distinguish the rocking curve from the fluctuations in a practicable time and keep the statistical error as low as possible. The rocking-curve measurement in the extinction position for a purity of $\delta_0 = 2.4 \times 10^{-10}$ has taken 2 h, for example. Because the path length of Bragg scattered and Compton scattered photons is different, one possibility to remove the Compton background is to discriminate the Compton scattered photons by time-gating of the detector, *i.e.* they can be ignored for the computation of the polarization purity. Alternatively, for future channel-cut designs the calculation of the beam path of Compton scattered photons should be included in the optimization procedure to avoid a deterioration of the purity, in particular for higher X-ray energies. It should also be kept in mind that Compton scattering in the monochromators may affect the monochromaticity and, thus, disturb the energy-sensitive measurements, although the distance between the monochromator and the experiment makes this fairly unlikely.

The remaining 12.3 photons s^{-1} caused by the higher harmonics cannot be identified by rocking-curve measurements and will limit the polarization purity if no other means to identify their origin as high harmonics are available. 12.3 photons s^{-1} against a total of 8×10^{9} photons s^{-1} then means a polarization purity of only 2×10^{-9}. For better purities, the harmonics need to be suppressed by a suitable monochromator detuning, total reflection at a glass plate or by detector discrimination.

5. Conclusion

We have measured 12 photons s^{-1} of high harmonics and 47 counts s^{-1} of Compton scattered photons in the spectrum of undulator radiation after passing a polarizer/analyzer setup close to the extinction position. We have shown that for sensitive polarization purity measurements the influence of the higher harmonics is not negligible and should, therefore, be suppressed. The effect of Compton scattered photons on the polarization purity could be avoided for the chosen crystal orientation, but it has to be kept in mind, in particular at high X-ray energies and for energy-sensitive experiments. These are two important new design criteria for ultra-high-definition X-ray polarimeters.

Acknowledgements

We would like to thank H. Marschner for crystal preparation. This work was supported by the German Science Foundation (DFG TR18) and the Carl-Zeiss-Stiftung.

References

Alp, E., Sturhahn, W. & Toellner, T. (2000). *Hyperfine Interact.* **125**, 45–68.
Hart, M. (1978). *Philos. Mag. B*, **38**, 41–56.
Hart, M. & Rodrigues, A. R. D. (1979). *Philos. Mag. B*, **40**, 149–157.
Heeg, K. P., Wille, H.-C., Schlage, K., Guryeva, T., Schumacher, D., Uschmann, I., Schulze, K. S., Marx, B., Kämpfer, T., Paulus, G. G., Röhlsberger, R. & Evers, J. (2013). *Phys. Rev. Lett.* **111**, 073601.
Heinzl, T., Liesfeld, B., Amthor, K.-U., Schwoerer, H., Sauerbrey, R. & Wipf, A. (2006). *Opt. Commun.* **267**, 318–321.
Kincaid, B. M. (1985). *J. Opt. Soc. Am. B*, **2**, 1294–1306.
Lai, B., Khounsary, A., Savoy, R., Moog, L. & Gluskin, E. (1993). Report ANL/APS/TB-3 ON: DE93008830. Argonne National Laboratory, IL, USA.
Marx, B., Schulze, K. S., Uschmann, I., Kämpfer, T., Lötzsch, R., Wehrhan, O., Wagner, W., Detlefs, C., Roth, T., Härtwig, J., Förster, E., Stöhlker, T. & Paulus, G. G. (2013). *Phys. Rev. Lett.* **110**, 254801.
Marx, B., Uschmann, I., Höfer, S., Lötzsch, R., Wehrhan, O., Förster, E., Kaluza, M., Stöhlker, T., Gies, H., Detlefs, C., Roth, T., Härtwig, J. & Paulus, G. (2011). *Opt. Commun.* **284**, 915–918.
Röhlsberger, R., Gerdau, E., Rüffer, R., Sturhahn, W., Toellner, T., Chumakov, A. & Alp, E. (1997). *Nucl. Instrum. Methods Phys. Res. A*, **394**, 251–255.
Siddons, D., Bergmann, U. & Hastings, J. (1999). *Hyperfine Interact.* **123–124**, 681–719.
Siddons, D., Hastings, J., Bergmann, U., Sette, F. & Krisch, M. (1995). *Nucl. Instrum. Methods Phys. Res. B*, **103**, 371–375.